Topology optimization of microbeams including layer deposition manufacturing constraints

<u>E. Lemaire</u>, V. Rochus, C. Fleury, J.-C. Golinval, P. Duysinx

University of Liège
Department of Mechanics and Aerospace
Institut de mécanique, Bat B52
Chemin des chevreuils 1, 4000 Liège Belgium
E.Lemaire@ULg.ac.be, P.Duysinx@ULg.ac.be

1. Abstract
As many manufacturing techniques, microfabrication methods possess limitations. Consequently, manufacturing constraints have to be considered during microsystems design process. Therefore, the direct use of automatic design tools like topology optimization is not possible. For instance, optimal topologies generally contain closed cavities that cannot be produced using the usual microfabrication techniques like layer deposition. The present paper intends to add a layer deposition constraint to the optimization problem using recent developments of *CONLIN* software. However, with this new optimization procedure we could observe that classical sensitivities filtering makes optimization problem rather unstable while filtering the density field itself keeps good convergence properties.
2. Keywords : Topology optimization, multiphysic, manufacturing constraint, microsystems

3. Introduction
Topology optimization has been widely applied during last years to problems involving one physical field (see [3, 2, 4, 6, 7, 14] for instance). The topology problem consists in distributing material in a fixed design volume in order to maximize a performance criterion given limited resources. The material distribution is represented mathematically by a density function equal to 1 where material is present and 0 in void areas. The privileged approach is based on a finite element discretization of the design domain. Usually, the density function is parameterized by attaching one design variable to each element. Then, the function is considered to be constant on each finite element. Nevertheless, the pure discrete problem suffers from non-existence of solution. Therefore, one solution is to relax the problem by allowing the density function to vary continuously between zero and one. Intermediate densities represent then either a porous material [3] whom properties are computed according to homogenization theory or an artificial material with mechanical properties given by an analytic law as the famous SIMP [2].

Because of the development of MEMS and their inherent multiphysic characteristics, the need for adaptation of optimization techniques to this field is constantly growing. However, the use of topology optimization for multiphysic problems is still under development. One of the first attempts to apply topology optimization to multiphysics systems was proposed by Sigmund [14]. Sigmund's objective was to use topology optimization to design electrothermal actuators in order to maximize the output point displacement. Yin and Ananthasuresh [17] have also studied these devices and have introduced an improvement of thermal convection modeling.

Later, topology optimization of electrostatic actuators has been studied by Raulli [11]. The approach proposed by Raulli is very general and gives a large design freedom to the optimizer. Even if the introduction of topology optimization complicates the staggered modeling, the resulting force inverters are very original and interesting.

An important phenomenon appearing in electrostatic actuators is pull-in effect. Indeed, these actuators possess a limit voltage called pull-in voltage beyond which they are unstable. Above a certain displacement and the corresponding voltage, elastic forces of suspension system cannot equilibrate electrostatic forces and electrodes stick together. This effect can eventually damage the actuator since it can be impossible to separate the electrodes afterward. In consequence pull-in limits the usable voltage range and it seems natural to use optimization methods in order to maximize the pull-in voltage. Abdalla *et al.* [1] initially propose and solve this optimization problem for microbeam with the help of a sizing technique. This method has been generalized recently by some of the authors in Ref. [9] using topology optimization. Moreover, a strongly coupled finite element formulation and a continuation procedure

were used in order to improve the modeling and sensitivity analysis exactness. Interesting and encouraging results were obtained. However, the final design lacks realism on a manufacturing point of view. Therefore, the main purpose of the present paper is to add a layer deposition manufacturing constraint to the optimization problem.

The paper is structured as follows. First, we recall the principles of the strongly coupled modeling and a path following algorithm, i.e. the normal flow, is adapted this formulation. Secondly, the optimization problem is described and we show how it is possible to evaluate its sensitivities. Then, we present the manufacturing constraint and justify its necessity. Finally, before the conclusions, applications are presented in order to highlight benefits and issues resulting from the manufacturing constraint introduction.

4. Strongly coupled modeling

Strongly coupled modeling methods are opposed to staggered or weakly coupled computation schemes in which each physical field of the model is solved separately. The advantage of weakly coupled modeling is the possibility to use existing modeling software for each physical problem whereas strong coupling requires for instance the development of a new finite element formulation. However, the ability of strongly coupled methods, also called monolithic, to solve all physical fields at the same time provides better convergence and stability properties than staggered procedures.

4.1. Electromechanical modeling

The modeling of electromechanical phenomenon as the pull-in effect occurring in microsystems is relatively difficult with a staggered algorithm. Therefore, a monolithic finite element formulation has been developed by Rochus (see reference [12]). To include both mechanical and electrostatic effects this formulation is based on the Gibbs energy density G given in equation (1). Gibbs energy density is constituted of two terms. The first one accounts for the mechanical energy contribution with the product of the stress tensor $\mathbf{S}$ by the strain tensor $\mathbf{T}$. The second term corresponds to the electric part of the energy and is equal to the product between the electric displacement $\mathbf{D}$ and the electric field $\mathbf{E}$.

$$G = \underbrace{\frac{1}{2}\mathbf{S}^T\mathbf{T}}_{mech.} - \underbrace{\frac{1}{2}\mathbf{D}^T\mathbf{E}}_{elec.} \tag{1}$$

Then, the application of a variational principle to the Gibbs energy density allows generating the finite element formulation. As a result, Rochus is able to compute the tangent stiffness matrix $\mathbf{K}_T$ of the complete multiphysic problem. Therefore, the linearized equilibrium equation linking generalized displacements increments $\Delta\mathbf{q}$ and generalized forces increments $\Delta\mathbf{g}$ can be written,

$$\mathbf{K}_T\Delta\mathbf{q} = \Delta\mathbf{g}$$

Where $\mathbf{q}$ the electromechanical degrees of freedom vector contains both mechanical displacements and electric potentials and $\mathbf{g}$ corresponds to the electromechanical generalized forces and collects mechanical forces and electric charges. Of course, the matrix $\mathbf{K}_T$ depends on the configuration $\mathbf{q}$.

4.2. Normal flow algorithm

Accurate knowledge of pull-in conditions is required by the sensitivity analysis. To solve this highly non linear problem, Rochus *et al.* in reference [12] propose to use a continuation algorithm in order to reach the pull-in point starting from the rest position. Continuation methods are similar to Newton-Raphson procedure since they consist in a succession of tangent predictions and correction phases. However, unlike Newton-Raphson, they introduce an additional load variable allowing the correction process to adjust the load applied to the system. The extra-variable requires an additional equation in order to keep a determined equation system. The choice of this equation depends on the continuation method. For instance, the normal flow method used in this paper (see references [1, 10]) constrains the corrections to be perpendicular to the *Davidenko flow* defined by the perturbed equilibrium equation,

$$\mathbf{r}\left(\mathbf{q}, \lambda\right) = \mathbf{f}_{ext} - \mathbf{f}_{int} = \boldsymbol{\delta}$$

where $\mathbf{r}$ is the residual forces vector, equal to the difference between external $\mathbf{f}_{ext}$ and internal $\mathbf{f}_{int}$ forces, $\boldsymbol{\delta}$ is any perturbation vector and λ is the load path variable. Figure 1 illustrates the normal flow iterative process. First a tangent step is performed starting form the equilibrium curve (continuous line) and secondly the correction phase restores the equilibrium condition following a path perpendicular to the *Davidenko flow* (dashed).
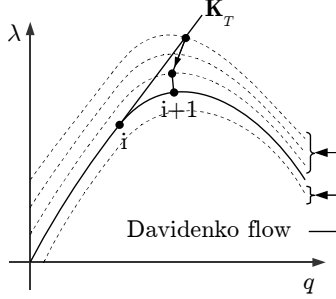

Figure 1: Normal flow method

As many non-linear solver, the normal flow method makes use of the linearized expression of the residual forces $\mathbf{r}$. Let's linearize $\mathbf{r}$ around the point $(\mathbf{q}_0, \lambda_0)$,

$$\mathbf{r}\left(\mathbf{q}_0 + \Delta\mathbf{q}, \lambda_0 + \Delta\lambda\right) \simeq \underbrace{\mathbf{r}\left(\mathbf{q}_0, \lambda_0\right)}_{\mathbf{r}_0} + \underbrace{\frac{\partial\mathbf{r}}{\partial\mathbf{q}}}_{-\mathbf{K}_T} \Delta\mathbf{q} + \frac{\partial\mathbf{r}}{\partial\lambda}\Delta\lambda \tag{2}$$

Since in this paper no external forces are considered, $\mathbf{r}$ is simply equal to the opposite of the internal forces. This is why we have,

$$\frac{\partial\mathbf{r}}{\partial\mathbf{q}} = -\frac{\partial\mathbf{f}_{int}}{\partial\mathbf{q}} = -\mathbf{K}_T \tag{3}$$

with $\mathbf{K}_T$ denoting the tangent stiffness matrix. Then, considering that we search $\Delta\mathbf{q}$ and $\Delta\lambda$ to zero $\mathbf{r}$, equation (2) can be rewritten,

$$\underbrace{\left[\begin{array}{cc} \mathbf{K}_T & -\frac{\partial\mathbf{r}}{\partial\lambda} \end{array}\right]}_{D\mathbf{r}} \underbrace{\left[\begin{array}{c} \Delta\mathbf{q} \\ \Delta\lambda \end{array}\right]}_{\Delta\mathbf{c}} = \mathbf{r}_0 \tag{4}$$

The perpendicularity condition is imposed by first computing the Davidenko flow tangent vector $\mathbf{u}$ defined by, $D\mathbf{r} \cdot \mathbf{u} = \mathbf{0}$. Therefore $\mathbf{u}$ can be computed by extracting the kernel of $D\mathbf{r}$. Then, the perpendicularity condition $\mathbf{u}^T \cdot \Delta\mathbf{c} = 0$ is introduced in the equation system (4), which finally gives,

$$\left[\begin{array}{cc} \mathbf{K}_T & -\frac{\partial\mathbf{r}}{\partial\lambda} \\ \mathbf{v}^T & \frac{d\lambda}{ds} \end{array}\right] \cdot \left[\begin{array}{c} \Delta\mathbf{q} \\ \Delta\lambda \end{array}\right] = \left[\begin{array}{c} \mathbf{r}_0 \\ 0 \end{array}\right]$$

if $\left[\mathbf{v}^T \, d\lambda/ds\right] = \mathbf{u}^T$ (s being a curvilinear abscissa).

In the context of an electrostatic actuator, it is logical to choose the applied voltage V as load variable. Notice that V corresponds to fixed electric potential degrees of freedom. In order to develop the expression of $\partial\mathbf{r}/\partial V$, we define $\mathbf{q}^i$ containing the imposed and fixed degrees of freedom of the model and $\mathbf{K}_T^{f,i}$ the part of the complete tangent stiffness matrix (i.e. before elimination) linking free degrees of freedom to imposed ones. Therefore since V only appears in $\mathbf{q}^i$ and not in $\mathbf{q}$, the derivative of $\mathbf{r}$ with respect to V can be written,

$$\frac{\partial\mathbf{r}}{\partial V} = \frac{\partial\mathbf{r}}{\partial\mathbf{q}^i}\frac{\partial\mathbf{q}^i}{\partial V} = -\mathbf{K}_T^{f,i}\frac{\partial\mathbf{q}^i}{\partial V} \tag{5}$$

Components of the vector $\partial\mathbf{q}^i/\partial V$ are equal to 1 if the corresponding degree of freedom is electric and imposed to V, otherwise they are zero.

Finally, notice that the unknown vector **c** contains both electrical and mechanical variables. Since MEMS usually experience voltages of at least 1 V and displacements about 1 μm, there exists a great magnitude dispersion of **c** components. Therefore, our experience has shown that the stability of the procedure was highly improved by normalizing the vector **c** such that all components are of the same order of magnitude.

5. Optimization problem

5.1. Description of the optimization problem

As shown by Raulli in Ref. [11] in the case of electromechanical coupling, the main difficulty of electromechanical optimization topology problems from the location of the electrostatic forces application point. These forces should normally be applied at the boundary between void and solid. However, in topology optimization this boundary is usually unclear since there is often a smooth transition between void and solid.

In this paper, in order to fix the electrostatic forces application point, we consider the reinforcement problem of a mobile electrode. Figure 2 represents the studied optimization problem. We can see in this figure that the mobile electrode, drawn in dark gray, separates the electric (in white) and optimization (in light gray) domains. Since, this electrode is non-optimizable, it prevents the optimization process to move the electrostatic forces application point. Moreover, as the mobile electrode is assumed perfectly conducting, the optimization domain is insulated from electrical effects and purely mechanical. Actually, the optimization problem consists in designing an optimal suspension for the mobile electrode. However, our optimization problem is still multiphysic and strongly non-linear since the interaction between mechanical and electric phenomena remains.
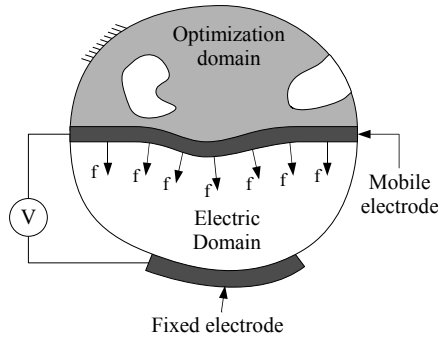

Figure 2: Schematic view of the considered optimization problem

The optimization problem considered is to maximize the pull-in voltage of an electromechanical device with a bound on the available volume of material. This can be mathematically stated as follow,

$$\max_{\boldsymbol{\mu}} V_{pi}(\boldsymbol{\mu}) \quad s.t. \begin{cases} v(\boldsymbol{\mu}) \leqslant \overline{v} \\ \mu_{min} \leqslant \mu_i \leqslant 1 \quad \forall i \end{cases}$$

where $\boldsymbol{\mu}$ represents the vector of design variables, $\overline{v}$ the upper bound on available material volume, $v(\boldsymbol{\mu})$ the structure volume and μ_{min} the lower bound on the unknowns.

The design material is an elastic-linear material under small strains assumption. In this study, we choose to model material behavior for non-integer densities using general homogenization laws for fiber composites proposed by Halpin and Tsai [8]. Considering a plane structure perforated by long fibers of very weak material perpendicularly to the plane of the structure, then according to Halpin-Tsai laws, the effective in plane Young's E modulus is given by the following equation in which ρ is the relative density of the material:

$$E = \frac{\xi\rho}{1 + \xi - \rho}E_0$$

The reinforcement parameter ξ can be modified in order to adjust the penalty on intermediate densities. A linear law is obtained for $\xi = \infty$ while the discrete problem is recovered for $\xi = 0$.

4

5.2. Sensitivity analysis

Considering the optimization problem stated above, it is possible to obtain an expression of the pull-in voltage sensitivities in function of the pull-in conditions. The sensitivities equation can be evaluated starting from the equilibrium equation by adapting the reasoning proposed by reference [1] to the strongly coupled formulation. Within the framework of this study, the equilibrium equation is written,

$$\mathbf{r}\left(\mathbf{q}, V\right) = \mathbf{f}_{ext} - \mathbf{f}_{int} = 0$$

where $\mathbf{r}$ stands for residual force vector, $\mathbf{q}$ are the generalized displacements and V is the applied electric potential. The equilibrium equation is then derived with respect to the design variable μ_i,

$$\frac{\partial \mathbf{r}}{\partial \mu_i} + \frac{\partial \mathbf{r}}{\partial \mathbf{q}} \frac{\partial \mathbf{q}}{\partial \mu_i} + \frac{\partial \mathbf{r}}{\partial V} \frac{\partial V}{\partial \mu_i} = \mathbf{0}$$

Notice that the perturbation of a design variable will not solely modify the structure pull-in voltage but also the deformation state at pull-in point. This is why, both derivatives of V and $\mathbf{q}$ with respect to μ_i have to be conserved. Adopting the notations of section 4.2. and using equations (3) and (5) the derivative of the residual forces becomes,

$$\frac{\partial \mathbf{r}}{\partial \mu_i} - \mathbf{K}_T \frac{\partial \mathbf{q}}{\partial \mu_i} - \mathbf{K}_T^{f,i} \frac{\partial \mathbf{q}^i}{\partial V} \frac{\partial V}{\partial \mu_i} = \mathbf{0} \tag{6}$$

Next, let's left multiply this equation by the first eigenvector $\mathbf{p}$ of $\mathbf{K}_T$. Since this matrix is singular at pull-in point we have $\mathbf{K}_T \mathbf{p} = \mathbf{0}$. In addition, the eigenvector is normalized to have,

$$\mathbf{p}^T \mathbf{K}_T^{f,i} \frac{\partial \mathbf{q}^i}{\partial V} = -1$$

Under this condition, the multiplication of (6) by $\mathbf{p}$ gives,

$$\mathbf{p}^T \frac{\partial \mathbf{r}}{\partial \mu_i} + \frac{\partial V_{pi}}{\partial \mu_i} = \mathbf{0}$$

As the optimization domain is purely mechanical, the variation of $\mathbf{r}$ resulting from a density perturbation comes solely from the mechanical contribution to the internal forces $\mathbf{f}_{int}$. This finally gives,

$$\frac{\partial V_{pi}}{\partial \mu_i} = \mathbf{p}^T \frac{\partial \mathbf{K}}{\partial \mu_i} \mathbf{q}$$

if $\mathbf{K}$ denotes the system linear stiffness matrix. In consequence, the sensitivities of pull-in voltage with respect to every variables requires only one pull-in search and the extraction of the first eigenmode of $\mathbf{K}_T$ at pull-in point.

5.3. Optimization problem regularization

As recalled in the introduction, the discrete topology optimization problem is ill-posed and the extension of design space to non entire densities is one possibility to obtain a well-posed problem. However this is not sufficient in general because mesh dependency problems can occur. Therefore, different solutions have been proposed as for instance perimeter constraint [7], sensitivity filtering [13] or density filtering [5, 6]. As this paper uses both sensitivity and density filters, these two methods are detailed here below.

5.3.1. Sensitivity filter

Inspired from image processing, sensitivity filtering was introduced in topology optimization by Sigmund [13]. The purpose of this method is to smooth the sensitivity field by using the following low pass filter,

$$\frac{\partial \hat{f}}{\partial \mu_i} = \frac{\sum_{j=1}^{N} \hat{H}_{ij} \mu_j \frac{\partial f}{\partial \mu_j}}{\mu_i \sum_{k=1}^{N} \hat{H}_{ik}} \quad \text{with} \quad \hat{H}_{ij} = \max\left(0, r_{max} - \text{dist}\left(i, j\right)\right)$$

The function $\text{dist}\left(i, j\right)$ provides the distance between elements i and j barycenters. Consequently, the sensitivity of each element is replaced by a weighted average of the sensitivities of elements included

in a neighborhood of radius r_{max}. This way, sensitivity filter prevents the appearance of checkerboard pattern and also introduces a minimum size constraint in the optimization problem. In spite of the heuristic nature of sensitivity filter, it has shown to provide good results and is widely used in topology optimization software.

5.3.2. Density filter

Another approach to regularize the optimization problem has been proposed by Bruns in reference [6]. Rather than filtering the sensitivities, Bruns proposes to average directly the densities. This means that the density ρ_k of an element is no more taken equal to only one design variable μ_i but is computed as a weighted average of the neighbor design variables. The expression of Bruns density filter is in fact similar to the sensitivity filter and is given by,

$$\rho_i = \frac{\sum_{j=1}^{N} \hat{H}_{ij}\mu_j}{\sum_{k=1}^{N} \hat{H}_{ik}} \quad \text{with} \quad \hat{H}_{ij} = \max\left(0, r_{max} - \text{dist}\,(i,j)\right) \tag{7}$$

where the operator $\text{dist}\,(i,j)$ represents the distance between the element i barycenter and the location of the variable μ_j (generally the element j barycenter). The sensitivities evaluation is then a little more sophisticated since a perturbation of the design variable μ_j influences several pseudo-densities. Therefore, $\partial f/\partial \mu_i$ is expressed as a linear combination of the $\partial f/\partial \rho_i$,

$$\frac{\partial f}{\partial \mu_j} = \sum_{i=1}^{N} \frac{\partial f}{\partial \rho_i}\frac{\partial \rho_i}{\partial \mu_j} = \sum_{i=1}^{N} \left(\frac{\partial f}{\partial \rho_i} \frac{\hat{H}_{ij}}{\sum_{k=1}^{N} \hat{H}_{ik}} \right)$$

As proved by Bourdin in Ref.[5], density filtering gives rise to a well-posed optimization problem. Moreover, the non-heuristic character of this method is its principal advantage on sensitivity filtering while the parameter r_{max} also allows introducing a minimum size constraint. One drawback of this filter is that the resulting topologies possess very smooth boundaries between void and solid. A few possibilities have been studied to remove gray material from the final design as bilateral filtering (see Ref. [16]) and image morphology operators (Ref. [15]).

5.4. Layer deposition constrain

The optimization procedure described provides interesting results. Figure 3 presents one application example of the method corresponding to the optimization of a simply supported microbeam. The design material is an isotropic quartz with a Young modulus $E = 86.79$ GPa and a Poisson ratio $\nu = 0.17$. The available volume of quartz is limited to 50% of the design domain volume and the material interpolation was performed using a Halpin-Tsai law of parameter 0.05. The design domain is meshed with 79 by 17 elements resulting in 1683 elements. A sensitivity filtering is applied with a radius 1.2 times the element size.

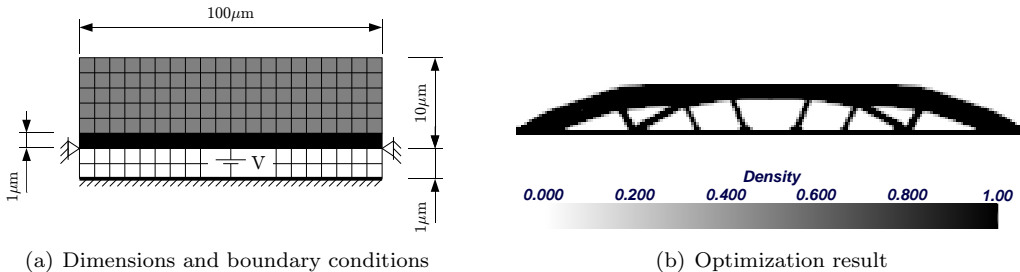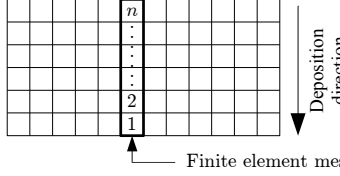(a) Dimensions and boundary conditions   (b) Optimization result

Figure 3: Topology optimization of pull-in without fabrication constraint

The bridge shaped result is common in topology optimization. However, closed cavities included into the structure are not suitable to classical MEMS layer deposition manufacturing process. In order to avoid the creation of those closed cavities, a fabrication constraint has been introduced. This fabrication

6

constraint is inspired from topology optimization of molded parts [18] where all cavities have to be opened in the same direction. The material deposition process used in MEMS imposes that all cavities have to be opened upward. Therefore, the deposition constraint is simply expressed by imposing decreasing densities when going upward in each column of the finite element mesh as stated in the following inequations for the column highlighted in the neighbor figure using the numbering given by the figure,

$$\begin{cases} 1 & \geqslant & \mu_1 & \geqslant & \mu_2 \\ \mu_{i-1} & \geqslant & \mu_i & \geqslant & \mu_{i+1} & \text{if} & 2 \leqslant i \leqslant n-1 \\ \mu_{n-1} & \geqslant & \mu_n & \geqslant & \mu_{min} \end{cases} \qquad (8)$$

This implementation results in an important number of linear constraints which increases the optimizer task difficulty. Therefore, different possibilities have been tested in order to avoid the use of linear constraints as replacing them by side constraints. But the use of side constraints is not enough flexible since it leads to a strong restriction of the design and causes optimization difficulties. However recent developments of *CONLIN* software allow handling this kind of constraint directly at the dual problem level without adding classical linear constraints. The applications of the present paper are solved using this new version of *CONLIN*.

6. Applications

6.1. Simply supported beam

In order to show the influence of the manufacturing constraint, we have chosen to apply it to the simply supported beam example presented in section 5.4. (see figure 3(a) for dimensions and boundary conditions). However with the new constraint, convergence to a 0-1 material distribution turned out to be difficult even with a strong penalty ($\xi = 0.01$ see figure 4(b)). In our mind this issue arises from the high sensitivities existing in the elements of the top of the domain (which results in the arch in figure 3(b)). Therefore the optimizer prefers to place intermediate density material higher in the optimization domain rather than placing unitary densities on the electrode. Nevertheless, we notice that replacing the uniform initial distribution by a shaded distribution (as shown in figure 4(a)) helps the optimizer and makes suppression of non-integer densities easier. With this initial distribution, a penalty coefficient $\xi = 0.1$ is sufficient to reach a (nearly) 0-1 distribution.

(a) Shaded initial distribution

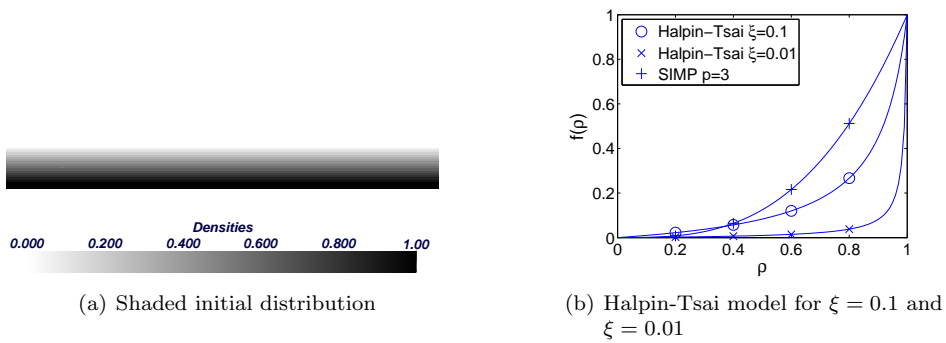(b) Halpin-Tsai model for $\xi = 0.1$ and $\xi = 0.01$

Figure 4: Dimensions and initial distribution of the first application

For this application and the following one, the stopping criteria of the optimization loop is based on the maximum variation of the design variables during optimization phase. We choose to stop the loop when this variations drops under 0.01. Finally, the minimal density ρ_{min} is set at 10^{-6}.

6.1.1. Sensitivity filter

At first, the optimization problem is regularized by using the sensitivity filter because the method has generally gives good results [4]. The filtering radius is taken equal to $r_{max} = 1.2 \times d$ where d is the finite

element size. However, after 13 iterations, the objective function begins to decrease at each optimization as shown in figure 5(a). From this iteration, the optimizer reduces elementary densities in large areas as illustrated in figure 5(b) where only one half of the domain is represented. This behavior is completely unexpected since we search to maximize the pull-in voltage. After a check of the sensitivities using finite differences, we have found that an increase of the filter radius makes the problem worse while a decrease has the opposite effect. In consequence, we have deactivated the regularization by setting the filter radius lower than elements size. The evolution curve obtained also presented in figure 5(a) shows a monotonous increase of the objective function. Therefore, this is most probably the association of the heuristic sensitivity filter with the new optimizer solver which generates the optimization troubles since without deposition constraint the sensitivity filter works properly as shown by the example in figure 3.
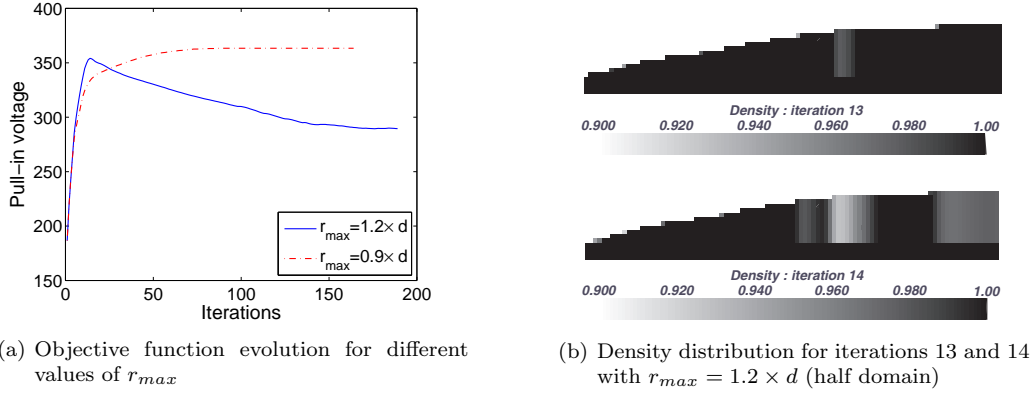

(a) Objective function evolution for different values of r_{max}

(b) Density distribution for iterations 13 and 14 with $r_{max} = 1.2 \times d$ (half domain)

Figure 5: Optimization results with sensitivity filtering and fabrication constraint activated (d being the elements size)

6.1.2. Density filter

Because mesh dependency problems can occur if the topology problem is not regularized, we choose to replace the sensitivity filtering by a density filtering (7). Density filtering has the advantage to be rigorous and relatively easy to implement. Figure 6 presents the optimal topology and the pull-in voltage evolution versus iteration for the current application with a filtering radius of $1.2 \times d$. The monotonous increase of the objective function and the well-converged resulting structure show the efficiency of the density filtering to avoid previous troubles while keeping the optimization problem well-posed.

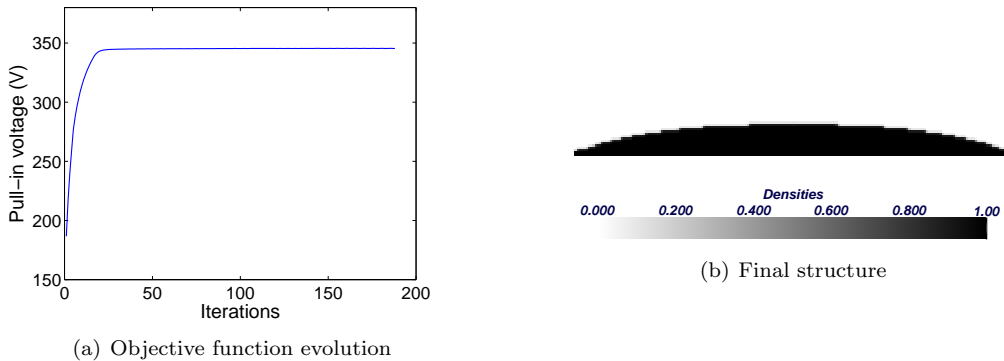(a) Objective function evolution

(b) Final structure

Figure 6: Optimization result with density filtering and fabrication constraint activated

The effect on the final structure of the fabrication constraint is clearly visible since no closed cavities are included in the microbeam. Nevertheless, the introduction of the manufacturing constraint reduces

strongly the optimal pull-in voltage. It decreases form 581 V (without constraint) to 345 V (with constraint) that is to say a loss of 41 %. Moreover, this good result requires an important computational cost. Indeed, even if the pull-in voltage doesn't evolve a lot during the last 150 iterations, these 188 iterations are necessary to obtain a structure with a regular and smooth profile.

6.2. Clamped-Simply supported beam

The second application aims to design an optimal suspension for the cantilever beam presented in figure 7(a). Fixations are now placed on the lower half of the mechanical domain left side while the fixed electrode lies solely under the right half of the mobile electrode. The amount of material is limited to 40 % of the design domain volume and the design material is identical to the previous application. The optimization domain is discretized with a mesh of 80 by 15 nodes resulting in 1027 design variables and the density filter has a radius of $1.2 \times d$. The penalty has to be higher in this case, ξ is set to 0.05.

(a) Dimensions and boundary conditions   (b) Optimization result
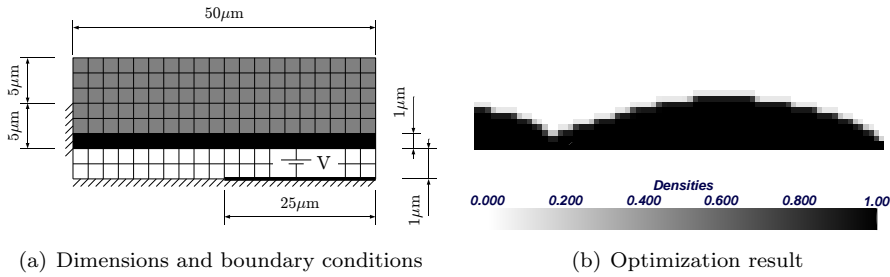
Figure 7: Clamped-Simply supported beam application

The resulting structure is presented on figure 7(b). This structure is divided in two parts by a hinge. The left part makes profit of the fixations available on this side and the right part reproduces a structure similar to the one obtained in the last application but not perfectly symmetrical this time. In fact, we can say that the left part generates at the position of the hinge a simple support on which the right part relies.

7. Conclusion and perspectives

The generality of topology optimization allows this method to design unexpected and original structures. Nevertheless, this generality may also become a drawback when considering the manufacturing of the optimization result. This is the case in the field of microsystems as illustrated above with the pull-in voltage topology optimization problem. Indeed, because of closed holes, the final structures are generally not compatible with the material deposition manufacturing process usually used in MEMS.

In this paper, a manufacturing constraint preventing the creation of closed holes has been added to the optimization problem. However, this constraint inspired from topology optimization of molded parts results in an important number of linear constraints and optimization problem by dual methods would be computationally too expensive. Nevertheless, the use of recent developments in *CONLIN* optimizer allows a fast and flexible treatment of this type constraint.

Unfortunately, we have observed that the new optimizer was incompatible with the regularization by sensitivity filtering. Indeed after a few iterations, the design variables updates performed by the optimizer become completely incoherent. Such problems arise most probably from the heuristic character of sensitivity filtering. Therefore, we have successfully replaced sensitivity filtering by a rigorous density filtering. The two applications proposed show that the method allows to obtain optimal structures without included cavities which are easier to manufacture using layer deposition.

In future work, one of the first tasks will be to allow the optimization process to modify the electro-static forces application point. This will have for consequence to remove the non-optimizable layer insulating the optimization domain from electric effect. Therefore, the optimization domain being electromechanical, the interpolation of the electric behavior will be required. This improvement will allow using completely the capabilities of topology optimization. In this context, the addition of the layer deposition constraint to the new problem will also be interesting.

8. Acknowledgment

9. References

[1] M.M. Abdalla, C.K. Reddy, W. Faris, and Z. Gurdal. Optimal design of an electrostatically actuated microbeam for maximum pull-in voltage. *Comp. & Struct.*, 83:1320–1329, 2005.

[2] M.P. Bendsøe. Optimal shape design as a material distribution problem. *Struct. Opt.*, 1:193–202, 1989.

[3] M.P. Bendsøe and N. Kikuchi. Generating optimal topologies in structural design using a homogenization method. *Comput. Methods Appl. Mech. Engrg.*, 71(2):197–224, 1988.

[4] M.P. Bendsøe and O. Sigmund. Topology optimization : theory, methods, and applications. *Springer Verlag*, 2003.

[5] B. Bourdin. Filters in topology optimization. *Int. J. Numer. Meth. Engng.*, 50:2143–2158, 2001.

[6] T.E. Bruns and D.A. Tortorelli. Topology optimization of non-linear elastic structures and compliant mechanisms. *Comput. Methods Appl. Mech. Engrg.*, 190:3343–3459, 2001.

[7] R.B. Haber, C.S. Yog, and M.P. Bendsøe. Variable-topology shape optimization with a control on perimeter. *Advances in Design Automation*, 69:261–272, September 1994.

[8] J.C. Halpin and S.W. Tsai. Effects of environmental factors on composite materials. *AFML-TR*, 67(423), June 1969.

[9] E. Lemaire, P. Duysinx, V. Rochus, and J.-C. Golinval. Improvement of pull-in voltage of electromechanical micorbeams using topology optimization. In *III European Conference on Computational Mechanics*, June 2006.

[10] S.A. Ragon, Z. Gurdal, and L.T. Watson. A comparison of three algorithms for tracing nonlinear equilibrium paths of structural systems. *Int. J. Solids Struct.*, 39:689–698, February 2002.

[11] M. Raulli and K. Maute. Topology optimization of electrostatically actuated microsystems. *Struct. & Mult. Opt.*, 30(5):342–359, November 2005.

[12] V. Rochus, D. J. Rixen, and J.-C. Golinval. Monolithic modelling of electro-mechanical coupling in micro-structures. *Int. J. Numer. Meth. Engng.*, 65(4):461–493, 2006.

[13] O. Sigmund. On the design of compliant mechanisms using topology optimization. *Mech. Struct. Mach.*, 25(4):493–526, 1997.

[14] O. Sigmund. Design of multiphysic actuators using topology optimization - Part I : One material structures. - Part II : Two-material structures. *Comput. Methods Appl. Mech. Engrg.*, 190(49–50):6577–6627, 2001.

[15] O. Sigmund. Morphology-based black and white filters for topology optimization. *Struct. & Mult. Opt.*, 33:401–424, January 2007.

[16] M. Y. Wang and S. Wang. Bilateral filtering for structural topology optimization. *Int. J. Numer. Meth. Engng.*, 63:1911–1938, April 2005.

[17] L. Yin and G.K. Ananthasuresh. A novel topology design scheme for the multi-physics problems of electro-thermally actuated compliant micromechanisms. *Sens. & Act.*, 97–98:599–609, April 2002.

[18] M. Zhou, R. Fleury, Y.K. Shyy, and H. Thomas ans J.M. Brennan. Progress in topology optimization with manufacturing constraints. In *9th AIAA/ISSMO Symposium on Mutlidisciplinary Analysis and Optimization*, Atlanta, Georgia, September 2002. AIAA.